Anti-VEGF single-chain antibody GLAF-1 encoded by oncolytic vaccinia virus significantly enhances antitumor therapy

Alexa Frentzen[a], Yong A. Yu[a], Nanhai Chen[a], Qian Zhang[a], Stephanie Weibel[b], Viktoria Raab[b], and Aladar A. Szalay[a,b,1]

[a]Genelux Corporation, San Diego Science Center, San Diego, CA 92109; and [b]Rudolph Virchow Center for Experimental Biomedicine, Institute for Biochemistry and Institute for Molecular Infection Biology, University of Würzburg, Am Hubland, D97074 Würzburg, Germany

Edited by George Klein, Karolinska Institute, Stockholm, Sweden, and approved May 28, 2009 (received for review January 20, 2009)

We previously reported that the replication-competent vaccinia virus (VACV) GLV-1h68 shows remarkable oncolytic activity and efficacy in different animal models as a single treatment modality and also in combination with chemotherapy [Yu YA, et al. (2009) *Mol Cancer Ther* 8:141–151]. Here, we report the construction of 3 VACV strains encoding GLAF-1, a previously undescribed engineered single-chain antibody (scAb). This unique scAb is transcribed from 3 vaccinia promoters (synthetic early, early/late, and late) and directed against both human and murine VEGFs. The expression of GLAF-1 was demonstrated in cell cultures. Also, the replication efficiency of all GLAF-1–expressing VACV strains in cell culture was similar to that of the parental GLV-1h68 virus. Successful tumor-specific delivery and continued production of functional scAb derived from individual VACV strains were obtained in tumor xenografts following a single intravenous injection of the virus. The VACV strains expressing the scAb exhibited significantly enhanced therapeutic efficacy in comparison to treatment of human tumor xenografts with the parental virus GLV-1h68. This enhanced efficacy was comparable to the concomitant treatment of tumors with a one-time i.v. injection of GLV-1h68 and multiple i.p. injections of Avastin. Taken together, the VACV-mediated delivery and production of immunotherapeutic anti-VEGF scAb in colonized tumors may open the way for a unique therapy concept: tumor-specific, locally amplified drug therapy in humans.

Avastin | GLV-1h68 | tumor colonization | angiogenesis | amplified drug therapy

Cancer is the leading cause of death following heart disease in the United States (1). There is a considerable ongoing research effort to find previously undescribed treatment options to expand the life expectancy of patients who have cancer or even to cure cancer completely.

In recent years, immunotherapy has emerged as an option for the treatment of cancer. Application of monoclonal antibodies has shown promising results in preclinical settings, and some have already reached the clinic. Nevertheless, the clinical use of monoclonal antibodies requires continued improvements. The generation of humanized monoclonal antibodies is very costly, and the antibodies' penetration into solid tumors after i.v. administration is limited because of high interstitial fluid pressure and limited diffusion (2, 3). Therefore, because of rapid clearance, high administration doses are needed to achieve high antibody concentration and local effects at the tumor site (4).

One of the most successful immunotherapeutic proteins is Avastin, which has been approved by the US Food and Drug Administration for use in combination with chemotherapy for treatment of metastatic colorectal cancer (CRC) and most forms of metastatic non-small cell lung cancer (NSCLC) (www.clinicaltrials.gov) (5). The mechanism of inhibition of angiogenesis has been extensively investigated in the past, and it is well established that Avastin has an inhibitory effect on the formation or maintenance of the tumor vasculature by binding human VEGF (6). Liang et al. (7) recently identified an antibody derived from a phage library that showed binding affinities even better than Avastin. Compared with Avastin, this G6–31 antibody showed enhanced efficacy in inhibition of tumor growth in different tumor models after i.p. administration (7). Furthermore, G6–31 treatment of tumors led to reduced blood vessel density (BVD) (7). It was suggested that, like Avastin, G6–31 causes inhibition of angiogenesis by sequestration of VEGF from its receptors on endothelial cells.

We have previously shown that the replication-competent vaccinia virus (VACV) GLV-1h68 leads to complete regression of solid tumors in nude mice as a single treatment after systemic or intratumoral delivery (8, 9). Nevertheless, in certain tumor types, virotherapy is limited if treatment solely relies on replication-mediated oncolysis. Recently, GLV-1h68 was also used in combination with chemotherapy, which enhanced the oncolytic effect beyond what was achieved using only the virus treatment (10). VACV exhibits advantages as an oncolytic virus. VACV has a large genome and a high capacity for recombinant gene delivery without compromising the oncolytic activity. It has also been shown to colonize tumor tissues selectively (11). GLV-1h68 is replication competent, which leads to high amplification in tumor tissue (8). Furthermore, because VACV is a cytoplasmically replicating DNA virus, integration into the host's genome is not possible. VACV was also found to be safe in humans in its previous application as a vaccine against smallpox (12).

In the current study, we showed that the combination of Avastin therapy with VACV GLV-1h68 oncolytic virotherapy led to a significant enhancement of tumor growth inhibition when compared with treatments with Avastin alone or the parental virus alone. We also generated a unique set of VACV strains that carried the single-chain antibody (scAb) sequence for the GLAF-1 protein, comprising the 2 variable domains of the therapeutic antibody connected by a linker sequence. The localized overexpression of the recombinant GLAF-1 protein was shown in tumor tissue, and the protein was also found in the circulation of tumorous mice. These previously undescribed VACV strains significantly enhanced the inhibition of tumor growth when compared with the parental GLV-1h68. Such growth inhibition data are comparable to concomitant treatment with separately injected Avastin and the parental virus GLV-1h68.

Results

Combination of Virotherapy with Avastin Treatment Leads to an Added Inhibitory Effect on Tumor Growth in Nude Mice. The oncolytic potency of GLV-1h68 alone and in combination with

Author contributions: A.F., Y.A.Y., N.C., Q.Z., and A.A.S. designed research; A.F., Y.A.Y., N.C., Q.Z., S.W., and V.R. performed research; A.F., Y.A.Y., N.C., Q.Z., S.W., V.R., and A.A.S. analyzed data; and A.F., Y.A.Y., N.C., Q.Z., S.W., and A.A.S. wrote the paper.

Conflict of interest statement: A.F., Y.A.Y., N.C., Q.Z., and A.A.S. are employees of Genelux Corporation.

This article is a PNAS Direct Submission.

[1]To whom correspondence should be addressed. E-mail: aaszalay@genelux.com.

This article contains supporting information online at www.pnas.org/cgi/content/full/0900660106/DCSupplemental.

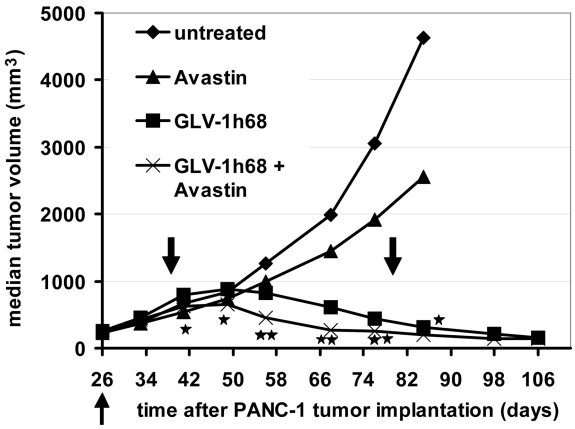

Fig. 1. Combination therapy of s.c. PANC-1 tumors with GLV-1h68 virus and Avastin. Tumor-bearing mice ($n = 8$ per group) were treated with the virus alone (5×10^6 pfu/mouse), with Avastin alone (5 mg/kg i.p. twice weekly for 5 weeks), with the virus initially (5×10^6 pfu/mouse) followed by Avastin treatment (5 mg/kg twice weekly for 5 weeks) 13 days later, or with no treatment. The up-pointing arrow indicates the time of virus injection. The down-pointing arrows indicate the beginning and end of Avastin treatment. Statistical analysis was performed using one-way ANOVA (**$P < 0.01$, *$P < 0.05$). Stars indicate the comparison of the GLV-1h68 group with the Avastin + GLV-1h68 group.

chemotherapy has been documented previously (8–10, 13, 14). To find out whether immunotherapy in combination with GLV-1h68 also leads to an enhanced growth inhibition of solid tumors, we treated PANC-1 tumor-bearing mice with Avastin alone, GLV-1h68 alone, or GLV-1h68 in combination with Avastin, using untreated tumors as controls. We found that Avastin alone led to slow and insignificant delays in tumor growth in comparison to untreated tumors (Fig. 1). After injection with GLV-1h68, we observed the characteristic 3-phase growth pattern described previously (8). In phase I, the tumor volume exceeded the volume of untreated tumors. Significant growth arrest was seen in phase II, followed by the continual regression of tumors over time (phase III). Injection of Avastin during virus treatment resulted in an added effect on tumor growth inhibition in comparison to virus-only treatment (Fig. 1). This effect could also be seen in the xenograft model MIA PaCa-2 [see supporting information (SI) Fig. S1]. Thus, we showed that the concomitant application of a single dose of i.v. virotherapy and multiple doses of i.p. immunotherapy gave better results than each treatment alone in the xenograft tumor models. Survival rates of mice are shown in Fig. S2 *B* and *C*. Overall survival rates among the different treatment groups are comparable.

VACV-Encoded Anti-VEGF scAb Protein Expressed in Infected A549 Cells Is Functional. Treatment of tumors with GLV-1h68 in combination with Avastin showed increased inhibition of tumor growth in comparison to GLV-1h68 treatment alone. To achieve intratumoral biosynthesis of proteins with an Avastin-like mode of action, 3 unique VACV strains were constructed. Each carries an expression cassette for the scAb GLAF-1, directed against human and murine VEGF. The expression cassette was inserted into the *J2R* locus of vaccinia genome downstream of synthetic early (SE), synthetic early/late (SEL), and synthetic late (SL) promoters, resulting in the GLV-1h107, GLV-1h108, and GLV-1h109 strains, respectively (Fig. 2 *A* and *B*). Several human carcinoma cell lines were infected with each of the individual recombinant virus strains, and the culture supernatants and cell lysates were tested for the presence of the GLAF-1 protein by

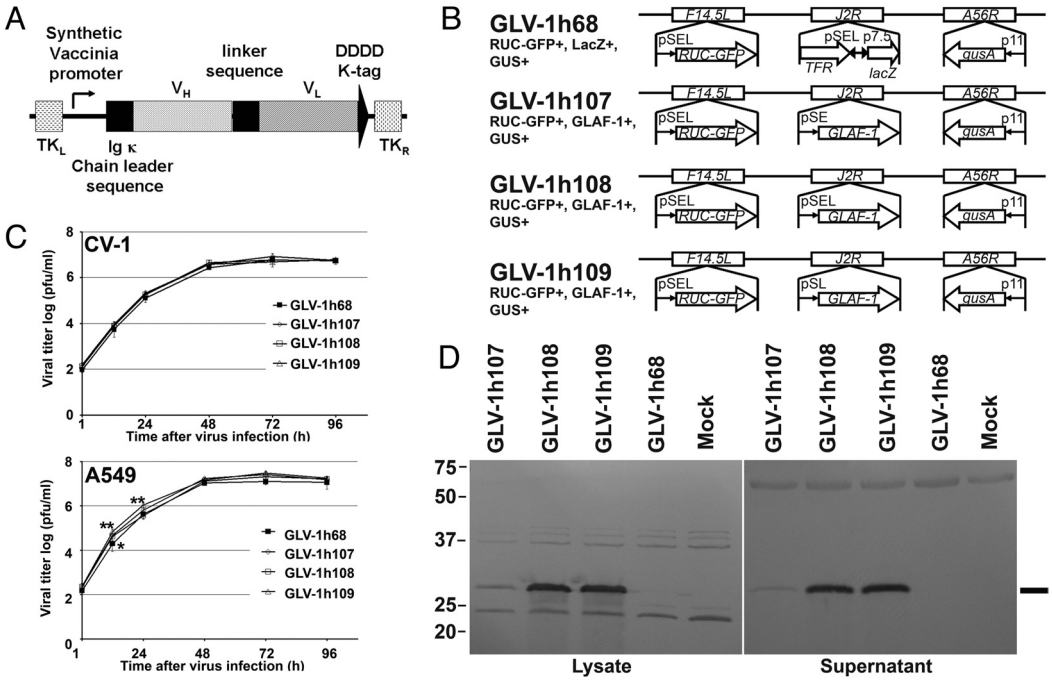

Fig. 2. Viral replication in A549 cells resulted in over-expression of the GLAF-1 scAb protein. (*A*) Schematic representation of the GLAF-1 scAb construct. (*B*) VACV constructs and marker genes. The LIVP WT virus strain was used for the generation of modified GLV-1h68 according to Zhang et al. (8). The GLV-1h68 virus was used for the construction of GLV-1h107, GLV-1h108, and GLV-1h109. p11, VACV p11 late promoter; pSEL, VACV SEL promoter; pSE, VACV SE promoter; pSL, VACV SL promoter; p7.5, VACV 7.5K early/late promoter. (*C*) Replication efficiency was determined after infection of CV-1 or A549 cells with VACV strains at an MOI of 0.01. Statistical analysis was performed using one-way ANOVA (**$P < 0.01$, *$P < 0.05$). Stars indicate comparison of the GLV-1h68 group with the groups of the unique viruses. (*D*) Expression of GLAF-1 in tumor cells in vitro. A549 cells were infected with VACV strains at an MOI of 1, and protein fractions from cell lysate and culture supernatant were isolated and separated by SDS/PAGE. Western blot analysis was performed using an anti-DDDDK antibody. The line shows the protein of the expected size of 30 kDa.

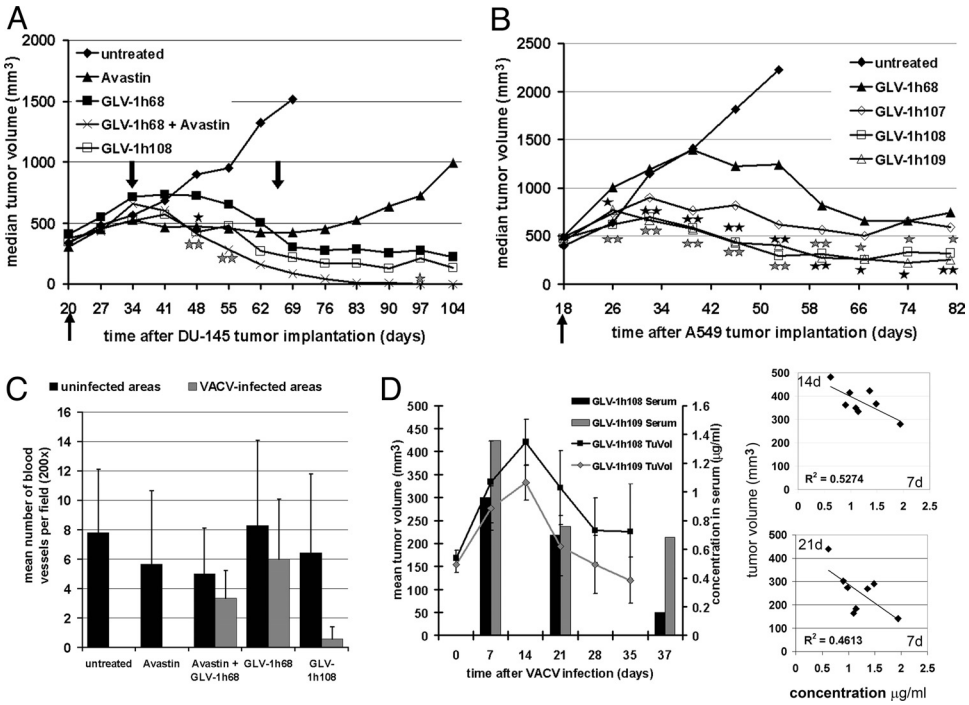

Fig. 3. GLAF-1 expression in GLV-1h108– and GLV-1h109–colonized tumors leads to enhanced tumor therapy and inhibition of BVD in mouse xenografts. (*A*) Therapeutic effect of VACV strains delivering GLAF-1 on tumor growth in DU-145 tumor-bearing nude mice ($n = 8$). The up-pointing arrow indicates the time of virus injection. The down-pointing arrows indicate the beginning and end of Avastin treatment. Statistical analysis was performed using one-way ANOVA (** $P < 0.01$, * $P < 0.05$). Stars indicate comparison of the GLV-1h68 group with the Avastin + GLV-1h68 group (gray) and the GLV-1h108 group (black). (*B*) Therapeutic effect of VACV strains delivering GLAF-1 on tumor growth in A549 tumor-bearing nude mice ($n = 7–8$). Statistical analysis was performed using one-way ANOVA (** $P < 0.01$, * $P < 0.05$). Stars indicate comparison of the GLV-1h68 group with the GLV-1h108 group (gray) and the GLV-1h109 group (black). (*C*) Quantitative analysis of BVD in DU-145 tumors 21 days after VACV infection. Data are given as means of cell number per high-power field (×200 magnification, $n = 3$) (*D*) Expression of GLAF-1 in sera and correlation of tumor volume changes of VACV-infected A549 tumor-bearing mice. Tumor fluid and retro-orbital blood samples were taken at days 7, 21, and 37 after virus injection from the same mice. Tumor growth was monitored by caliper measurements. Protein amounts were quantitatively determined by ELISA with VEGF-precoated plates. Experimental groups contained 4 animals each.

Western blot analysis. A representative example of infected human lung carcinoma A549 cells is shown (Fig. 2*D*). GLV-1h107–, GLV-1h108–, and GLV-1h109–infected A549 cells showed a specific protein of the expected size of 30 kDa (Fig. 2*D*). No protein of similar size was detected in uninfected cells or cells infected with the parental virus GLV-1h68, without the expression cassette (Fig. 2*D*). The expression levels of the GLAF-1 proteins in cell lysates and culture supernatants were found to be lowest in GLV-1h107–infected cells and of comparable strength in GLV-1h108– and GLV-1h109–infected cells (Fig. 2*D*) (15).

Overexpression of GLAF-1 Protein in Infected A549 Cells Do Not Interfere with Efficiency of Virus Replication. To investigate whether GLAF-1 scAb protein expression altered the replication efficiency in comparison to the parental virus without GLAF-1, CV-1 or A549 cells were infected with all 3 unique VACV strains at a multiplicity of infection (MOI) of 0.01, followed by determination of viral titers at different time points postinfection (p.i.). In CV-1 cells, no difference in replication efficiency could be found (Fig. 2*C*). Unexpectedly, GLV-1h107, GLV-1h108, and GLV-1h109 showed enhanced replication efficiency in A459 cells 12 h p.i., in comparison to the parental virus GLV-1h68. After 24 h, only the VACV strains GLV-1h108 and GLV-1h109 showed significantly higher replication efficiency than GLV-1h68 in this cell line. Taken together, data obtained at all time points did not show any negative effects on overall replication efficiency (Fig. 2*C*).

GLAF-1 scAb Protein Is Present in Colonized Tumor Xenografts and in Sera of Mice. After demonstration of GLAF-1 scAb protein expression in cell cultures, the presence of the anti-VEGF scAb in tumorous mice was also investigated. Mice harboring A549 tumor xenografts of ≈250 mm^3 in size were injected i.v. with GLV-1h68, GLV-1h108, and GLV-1h109. Seven, 21, and 37 days p.i., tumor fluid samples were taken along with serum isolation from blood samples. All samples were analyzed further for binding of GLAF-1 scAb to human VEGF-precoated microtiter plates. Fig. 3*D* shows that GLAF-1 could be readily detected 7 days p.i. in the serum of GLV-1h108– and GLV-1h109–infected tumor-bearing mice. Corresponding tumor fluid samples showed that the expression of GLAF-1 in infected areas of tumors was 12 (12 μg/mL) and 15 (20 μg/mL) times higher in GLV-1h108– and GLV-1h109–infected mice, respectively, in comparison to sera. There was a negative correlation between the tumor volume at day 14 and day 21 p.i. and the sera concentration of GLAF-1 at day 7. These findings suggest that higher GLAF-1 expression at an early stage (day 7) results in a smaller tumor size at day 14 or day 21 (Fig. 3*D*, *Right*). Over time, the concentration of GLAF-1 in the sera of treated mice gradually decreased (Fig. 3*D*, *Left*).

Tumor Regression Is Pronounced in GLAF-1 Overexpressed Xenografts. To investigate the contribution of the GLAF-1 scAb protein to tumor progression, DU-145 or A549 tumor-bearing nude mice were injected i.v. with the VACV strains GLV-1h68 and GLV-1h108 or with GLV-1h68, GLV-1h107, GLV-1h108, and GLV-1h109, respectively. Tumorous mice with no virus infection were used as negative controls. In case of DU-145 tumorous mice, a group of uninfected and GLV-1h68–infected mice were treated with Avastin twice weekly for 5 weeks, starting at day 14. In both models, rapid tumor growth was observed in control mice (Fig.

3 *A* and *B*). In GLV-1h68–treated animals, the tumor growth exhibited the typical 3-phase growth pattern, as described previously. Fig. 3*A* shows that the median DU-145 tumor volume changed following i.v. injection of the different viruses and Avastin treatment. Treatment with Avastin alone led to stagnation in tumor growth for the period of the Avastin administrations, followed by an increase in tumor volume after the termination of treatment. The concomitant treatment of GLV-1h68 and Avastin in mice led to an enhanced regression of tumor growth, in comparison with GLV-1h68 treatment alone, followed by complete regression. GLV-1h108–treated tumors showed an intermediate inhibitory effect between GLV-1h68 and the combination therapy (Fig. 3*A*). Fig. 3*B* shows the median A549 tumor volume changes following i.v. injection of the different recombinant viruses. Tumorous mice treated with GLV-1h107 showed an immediate and overall inhibition of tumor growth when compared with the GLV-1h68 treatment group (Fig. 3*B*). Fourteen days after virus injection, the regression phase had already started, much sooner than in the GLV-1h68 treatment group. In tumorous mice treated with GLV-1h108 and GLV-1h109, the inhibition of tumor growth was even more dramatic than in mice treated with GLV-1h68. In the GLV-1h108 and GLV-1h109 groups, tumor growth was arrested very soon after virus injection and did not reach the tumor sizes observed in GLV-1h68–treated mice during the inhibitory phase. Over the course of therapy, tumor sizes in GLV-1h108 and GLV-1h109 virus-treated mice remained significantly smaller than those of GLV-1h107 virus-treated mice. At the end point of the experiment, median tumor volumes of these mice were much smaller than those in GLV-1h68–treated animals. Based on net body weight change data, the toxicity profiles of GLV-1h107 and GLV-1h109 were comparable to that of GLV-1h68 throughout the study. GLV-1h108 showed an increased toxicity in comparison to GLV-1h68 (Fig. S2*A*). Experiments monitoring the biodistribution of VACV in different organs of mice showed that all 3 unique VACV strains are rapidly cleared from all organs except tumors, as previously described for GLV-1h68 (8), and that all 3 unique recombinant VACV strains exhibited similar tumor specificity (Table S1).

DU-145 and A549 Tumors Colonized by GLAF-1–Expressing Viruses Exhibit Drastically Reduced BVD. We have shown previously in this article that the GLAF-1 scAb was detected in tumors colonized by GLAF-1 highly expressed virus strains. The inhibitory effect of the expressed GLAF-1 scAb on the tumor vasculature, as hypothesized, was evaluated in tumor sections by immunohistochemistry (IHC). DU-145 tumors were excised on day 21 p.i., and BVD was determined by blood vessel counts after staining the vessels for the presence of PECAM-1 (CD31). Also, the level of VACV infection was determined by immunohistochemical staining of a VACV-specific antigen (Fig. 3*C* and Fig. S3). Fig. 3*C* shows the mean BVD in uninfected and infected areas of tumors. Uninfected areas of virus-treated tumors did not show significant differences when compared with untreated tumors. However, in infected areas of tumors, significant differences in BVD were observed (Fig. 3*C*). The concomitant treatment of Avastin and GLV-1h68 led to a slightly reduced BVD when compared with GLV-1h68 treatment alone. When treated with GLV-1h108, a dramatic reduction of BVD was observed in infected areas, which correlated with more advanced necrosis in these tumors in comparison to GLV-1h68–treated tumors (Fig. 3*C* and Fig. S3). Representative images of the different treatment groups are shown in Fig. 4, visualized by fluorescence stereomicroscopy. In an additional experiment, VACV-treated A549 tumors were excised on day 7 after virus injection and the CD31-positive tumor vasculature was analyzed in tissue sections by fluorescence stereomicroscopy (Fig. S4). The results were similar to data shown in Fig. 4. Thus, we concluded that

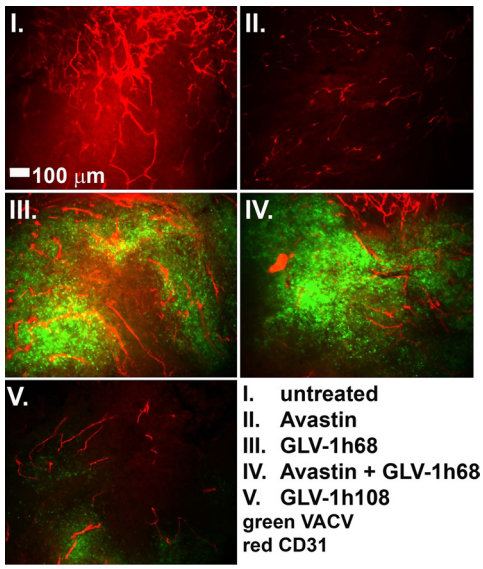

Fig. 4. Effect of virus treatment on tumor vasculature in DU-145 tumors. Tumors were excised at day 21 p.i., fixed, sectioned, and stained for CD31 to label endothelial cells (red). GFP expression indicates viral infection (green). All images are representative examples. (Scale bar: 100 μm.)

colonization of tumors with GLAF-1–expressing VACV strains resulted in significant inhibition of the development or maintenance of tumor vasculature.

Discussion

It has previously been demonstrated that VACV is a promising candidate for oncolytic virotherapy of solid tumors in human tumor xenograft models in mice (8, 9, 16–18). In these approaches, complete tumor regression was achieved over a period after a single systemic dose of GLV-1h68 (8). In addition, the already superior virus GLV-1h68 showed enhanced and accelerated efficacy in combination with chemotherapy in pancreatic cell lines and tumors (10). Here, we report the generation of 3 derivatives of the GLV-1h68 virus by replacing into the *J2R* locus an expression cassette encoding the previously undescribed anti-VEGF scAb GLAF-1 protein, which was designed to bind both human and murine VEGF. We designed experiments to study VACV-mediated and scAb-facilitated oncolytic virotherapy and immunotherapy in virus-colonized tumors.

We showed that GLAF-1 was expressed in virus-infected tumor cells in cell culture and in colonized human lung cancer xenografts in nude mice. The virus-encoded scAb GLAF-1 led to an enhanced therapeutic effect in different human tumor xenograft models, compared with oncolytic viral therapy with GLV-1h68 alone. This enhancement may be caused by the continuous production of the anti-VEGF scAb in colonized tumors. The previously undescribed recombinant viruses showed low toxicity and unaltered replication efficacy. Thus, the insertion of the therapeutic gene cassette into the viral genome did not negatively affect the previously seen oncolytic virotherapeutic efficacy.

It is well established that continuous tumor progression requires neoangiogenesis (19). High levels of VEGF in patients who have cancer have been associated with a less favorable prognosis of treatment outcome (20). Therefore, inhibiting vascularization of tumors has been extensively studied (21, 22). Despite very promising preclinical results, Avastin has not shown the potent clinical success expected in patients when used in combination with chemotherapy for the treatment of metastatic CRC and NSCLC (23). The lack of efficacy of Avastin in

combination therapy may be attributable to the poor penetration of the antibody into the tumor tissue from the blood after systemic treatment. Therefore, high doses of the antibody protein were necessary to achieve a more significant effect. Here, we showed that treatment with GLV-1h68 and Avastin led to improved oncolytic vibrotherapy, and thus demonstrated that the combination of oncolytic virotherapy and immunotherapy may be feasible as a previously undescribed strategy to treat cancers. We also showed that the unique recombinant VACV strains harboring the *GLAF-1* gene with different promoters exhibited enhanced tumor inhibition and therapeutic potency, which was comparable to the results seen in combination therapy with separately applied Avastin and GLV-1h68. The GLAF-1 protein was designed based on the partial sequence of the antibody G6–31, which was previously shown to bind both murine and human VEGF with high affinity (7). The binding to VEGF from both human and mouse origins is advantageous in the human tumor xenograft model in mice, because inhibition of VEGF from a murine stromal origin in the tumor was important for therapeutic efficacy (24). The efficient binding of the unique scAb GLAF-1 to VEGF was also confirmed in this system.

We demonstrated infection and replication of the GLAF-1–encoding recombinant VACV strains at the tumor site and, more importantly, localized expression of the GLAF-1 scAb protein in colonized tumors. This localized expression of the GLAF-1 scAb led to marked inhibition of the tumor growth in mice. The continuous biosynthesis of the therapeutic scAb was coupled with successful replication of the virus in tumors. Thus, the presence of GLAF-1 protein in the circulation may result in a continuous therapeutic process at previously uninfected sites without the need for repeated injections of a therapeutic agent. This continuous delivery system will terminate once the tumor regression is completed and the colonizing virus particles are also eliminated from the tumor site by the immune system (8). Thus, no long-term inhibitory effects would be expected in the absence of the virus on GLAF-1 expression-mediated oncolytic virotherapy.

The IHC analysis of the tumors showed a reduction of tumor BVD in virus-infected areas in tumors at different time points after treatment with GLV-1h108 in the tumor models examined. Further, GLAF-1 displayed significant inhibitory effects on tumor blood vessel development and maintenance, similar to the previously described protein G6–31 (7). Depending on the xenograft model, the replication levels of VACV in the tumor tissue seemed to be altered. Therefore, the inhibitory effect of GLAF-1 paralleled the extent of replication of VACV over time. These effects are tumor specific and correlated with the extent of inhibition of neoangiogenesis. Such inhibition may offer a therapeutic window of slowed tumor growth that allows the oncolytic virus to destroy the tumor cells more efficiently. A direct comparison of the efficacy of the i.v. injected Avastin (human-specific) with the intratumorally produced GLAF-1 (against both human and murine VEGF) is not appropriate.

Because the inhibition of VEGF may lead to up-regulation of other growth factors involved in neoangiogenesis mechanisms (25–27), response mechanisms to antiangiogenic treatment after anti-VEGF scAb treatment need further investigation. Oncolytic viral therapy could potentially be used alongside antiangiogenic treatment, because viral therapy demonstrated long-lasting inhibition and regression of tumor growth.

Tumor therapy results indicated that tumor growth inhibition by the 3 unique recombinant viruses with GLAF-1 expression was directly proportional to promoter strength driving the *GLAF-1* gene expression (15). Strain GLV-1h107 carries the SE promoter, whereas GLV-1h108 and GLV-1h109 both harbor the much stronger SEL and SL promoters, respectively. The promoter strength was verified by direct comparison of the expression levels of GLAF-1 in cell cultures. Consequently, the best antitumor effects were obtained with GLV-1h108 and GLV-1h109 treatment of tumors.

It was also reported that VEGF and other angiogenic factors are involved in tumor immune evasion (28, 29). VEGF has been shown to act as an immunosuppressant (30). It is not clear at this time whether the overexpression of GLAF-1 scAb has an effect on the immune system. The infection of tumors with VACV leads to activation of the innate immune system at the tumor site (8). On infection with VACV, the tumor growth-supporting microenvironment may shift to an antitumor growth environment that includes the recruitment of important immune effector cells (31, 32).

In conclusion, the data presented here clearly show that the VACV-encoded anti-VEGF scAb GLAF-1 significantly improved tumor therapy in xenografts. This effect is superior to GLV-1h68 oncolytic therapy alone, which, in turn, was far superior to Avastin therapy alone in the same model systems. We also showed that the expression of an anti-VEGF scAb can be achieved after colonization of tumors with VACV. Therefore, we propose that tumor colonization in combination with efficient intratumoral replication and VACV-mediated therapeutic gene overexpression is a previously undescribed continuous therapeutic system. These findings also establish the concept of using tumors as drug factories in the fight against cancer.

Materials and Methods

Cell Lines. African green monkey kidney fibroblasts (CV-1), the human pancreatic ductal carcinoma cell line PANC-1, the human pancreatic carcinoma MIA PaCa-2, the human prostate carcinoma DU-145, and the human lung carcinoma A549 were obtained from the American Type Culture Collection. CV-1, PANC-1, or MIA PaCa-2 cells were cultured in DMEM supplemented with 1× antibiotic-antimycotic solution (100 U/mL penicillin G, 250 ng/mL amphotericin B, and 100 U/mL streptomycin) and 10% or 12.5% (vol/vol) FBS (Invitrogen Corporation), respectively. DU-145 cells were cultured in Eagle's minimal essential medium (EMEM) supplemented with 10% (vol/vol) FBS, 1× antibiotic-antimycotic solution, 1% sodium pyruvate, and 1% non-essential amino acids (NEAA). A549 cells were cultured in RPMI 1640 supplemented with 10% (vol/vol) FBS and antibiotic-antimycotic solution.

Construction of Plasmids and Recombinant VACV Strains. Standard cloning techniques were used for the construction of plasmids. The plasmid 0608997-pGA4 was synthesized by GENEART AG and contains a fragment coding for the single chain anti-VEGF antibody GLAF-1, comprising an Igκ light chain leader sequence (34), the V_H chain sequence of the G6 Fab (7), a $(G_4S)_3$ linker sequence, the V_L chain sequence of the G6 Fab (7), and a C-terminal DDDDK sequence (Fig. 2*A*). To construct the final plasmids, the VACV DNA homology-based shuttle plasmids pCR-TK-P_{SE}, pCR-TK-P_{SEL}, and pCR-TK-P_{SL} were used, which were previously constructed for homologous recombination of foreign genes into the *J2R* locus in the VACV genome through double reciprocal crossover. The *GLAF-1* fragment was cloned into the framework plasmids via the SalI and PacI sites, resulting in the plasmids pCR-TK-P_{SE}-*GLAF-1*, pCR-TK-P_{SEL}-*GLAF-1*, and pCR-TK-P_{SL}-*GLAF-1*.

The recombinant viruses GLV-1h107, GLV-1h108, and GLV-1h109 contain the *GLAF-1* gene under the control of the VACV SE, SEL, and SL promoters, respectively. These were inserted at the *J2R* locus and were constructed from the parental virus GLV-1h68. The recombinant viruses were constructed as previously described (34). Recombinant viruses were propagated in CV-1 cells and purified through sucrose gradients (35). Fig. 2*B* shows a schematic overview of the VACV constructs and marker gene locations in the genome.

The triple-mutant GLV-1h68 virus was constructed and described previously (8). GLV-1h68 contains 3 expression cassettes (encoding *Renilla* luciferase-*Aequorea* GFP fusion protein, β-galactosidase, and β-glucuronidase) integrated into the *F14.5L*, *J2R*, and *A56R* loci of the LIVP viral genome, respectively.

Viral Proliferation Assay. Standard plaque assays were used to quantify viral replication following infection with the different recombinant VACV strains. CV-1 and A549 lung cancer cells were infected with VACV at an MOI of 0.01, and cells were harvested after time points 1, 12, 24, 48, 72, and 96 h p.i. Cells were lysed by applying 3 freeze/thaw cycles followed by sonication. Serial dilutions cultured on confluent layers of CV-1 cells in 24-well plates and titers were determined 48 h later.

GLAF-1 Protein Expression. A549 cells were infected with virus at an MOI of 1. Both culture supernatants and cell lysates were harvested 24 and 48 h p.i. Protein fractions were denatured, separated via vertical SDS-PAGE, and transferred to a PVDF-membrane. The recombinant protein was bound via a rabbit anti-DDDDK antibody (Abcam) and detected via an HRP-conjugated anti-rabbit IgG (Jackson Immuno Research) and the chromogenic detection kit Opti4CN (Bio-Rad).

The expression of the recombinant proteins in tumor fluid and sera in vivo was tested by ELISA assays. Ninety-six–well plates precoated with recombinant human VEGF (Sigma) were blocked and incubated with sera and tumor fluid samples in 1:20 and 1:100 dilutions, respectively. Following a 1.5-h incubation at room temperature, the wells were washed with PBS/0.05% Tween and incubated with a rabbit anti-DDDDK antibody (Abcam) and then washed and incubated with a secondary HRP-conjugated anti-rabbit IgG (Jackson Immuno Research). Color was developed using 3,3,5,5′-tetramethylbenzidine (Sigma), and the reaction was stopped by adding 2 M HCl. Absorbance was read in a microplate reader at 450 nm. The GLAF-1 protein was obtained by infecting CV-1 cells with GLV-1h108 for 24 h at an MOI of 10. Supernatants were concentrated by centrifugation with centrifugal filter units (Millipore), followed by purification using the FLAG Tagged Protein Immunoprecipitation Kit (Sigma). Purification was verified using Coomassie gel analysis, and concentrations were measured with the Bio-Rad DC Protein Assay (Bio-Rad).

Animal Models and Tumor Therapy in Vivo. Five- to 6-week-old female or male Hsd:athymic Nude-*Foxn1*^{nu} mice (Harlan) were implanted s.c. with either 5×10^6 of A549 or PANC-1 cells or with 1×10^7 of DU-145 or MIA PaCa-2 cells into the lateral right thigh. After tumor growth reached a size of approximately 250 mm^3 (450 mm^3 for DU-145), mice were injected i.v. with the different VACV strains at 5×10^6 pfu/mouse (2×10^6 pfu/mouse for DU-145). For the Avastin treatment, mice were injected i.p. with 5 mg/kg Avastin (Genentech/Roche) twice weekly for 5 weeks starting at day 13 after virus injection. Tumor growth was measured over time using a digital caliper to evaluate the therapeutic efficacy. The following formula was used to calculate the tumor volume: [(height − 5 mm) × width × length]/2. Toxicity of the viruses was assessed by monitoring relative weight changes of the animals. Samples for the protein expression analysis in ELISA (see above) were taken at time points 7, 21, and 37 days by poking tumors with a 27-gauge needle and extracting tumor fluid as well as by drawing blood from the retro-orbital venous plexus.

Mice were cared for and maintained in accordance with animal welfare regulations under the approved protocol by the Institutional Animal Care and Use Committee of LAB Research International, Inc. and Explora Biolabs (San Diego Science Center).

Histology. Histological studies were conducted as previously described (36). Briefly, tumors were excised 7 days and 21 days p.i., snap-frozen for 5 min in liquid N_2, and embedded in paraffin. Paraformaldehyde-fixed tumors were cut into 100-μm sections. Specimens were then labeled with anti-CD31 antibody (BD PharMingen) for 12 h, followed by incubation with Cy3-conjugated donkey anti-rat antibody (Jackson ImmunoResearch) for 5 h. The examination of the tumor sections was conducted with an MZ16 FA fluorescence stereomicroscope (Leica) equipped with a digital CCD camera (Leica). GFP expression of virus-infected cells and CD31 expression in tumor sections were monitored. Digital images (1,300- × 1,030-pixel images) were processed using Adobe Photoshop 7.0 software. Paraffin-embedded tissue was cut into 5-μm sections, and H&E staining was performed. Adjacent slides were stained for the presence of PECAM-1 and VACV, respectively. Antigen retrieval was performed with citrate buffer. For PECAM-1 staining, tissue was blocked with normal rabbit serum, peroxidase treated, incubated with anti-PECAM-1 (Santa Cruz Biotechnology), and then incubated with a rabbit anti-goat IgG as a secondary antibody (Vector Laboratories). For the VACV staining, tissue was blocked with normal goat serum, peroxidase treated, and incubated with an anti-A27L antibody custom-made against a VACV synthetic peptide (GenScript Corporation). A goat anti-rabbit IgG was used as a secondary antibody (Vector Laboratories). Detection was performed with Vectorstain Elite ABC reagent and Vector ImmPact DAB Peroxidase substrate (Vector Laboratories). Sections were counterstained with hematoxylin. Quantitative analysis of microvessel density was made by counting positively stained cells in 10 high-power fields (×200) according to Weidner et al. (37).

Statistical Analysis. Statistical analyses were performed with SPSS, version 11 (SPSS, Inc.). Comparisons of treatment groups were made by ANOVA, and the differences between the groups were analyzed with an least significant difference (LSD) test when the ANOVA showed an overall significance. Values of P less than 0.05 were considered significant.

ACKNOWLEDGMENTS. We thank Terry Trevino, Melody Jing, and Ulrike Geissinger for excellent technical support and Andrea Feathers for editorial support. This work was supported by grants from Genelux Corporation (R&D facility in San Diego, CA). The authors would like to dedicate this paper to Dr. Robert L. Sinsheimer (Chancellor Emeritus and Professor).

1. American Cancer Society (2008) *Cancer Facts and Figures 2008* (American Cancer Society, Atlanta).
2. Jain RK (1989) Delivery of novel therapeutic agents in tumors: Physiological barriers and strategies. *J Natl Cancer Inst* 81:570–576.
3. Jain RK (2001) Delivery of molecular and cellular medicine to solid tumors. *Adv Drug Delivery Rev* 46:149–168.
4. Reilly RM, et al. (1995) Problems of delivery of monoclonal antibodies. Pharmaceutical and pharmacokinetic solutions. *Clin Pharmacokinet* 28:126–142.
5. Manegold C (2008) Bevacizumab for the treatment of advanced non-small-cell lung cancer. *Expert Rev Anticancer Ther* 8:689–699.
6. Willett CG, et al. (2004) Direct evidence that the VEGF-specific antibody bevacizumab has antivascular effects in human rectal cancer. *Nat Med* 10:145–147.
7. Liang WC, et al. (2006) Cross-species vascular endothelial growth factor (VEGF)-blocking antibodies completely inhibit the growth of human tumor xenografts and measure the contribution of stromal VEGF. *J Biol Chem* 281:951–961.
8. Zhang Q, et al. (2007) Eradication of solid human breast tumors in nude mice with an intravenously injected light-emitting oncolytic vaccinia virus. *Cancer Res* 67:10038–10046.
9. Lin SF, et al. (2008) Oncolytic vaccinia virotherapy of anaplastic thyroid cancer in vivo. *J Clin Endocrinol Metab* 93:4403–4407.
10. Yu YA, et al. (2009) Regression of human pancreatic tumor xenografts in mice after a single systemic injection of recombinant vaccinia virus GLV-1h68. *Mol Cancer Ther* 8:141–151.
11. Yu YA, Timiryasova T, Zhang Q, Beltz R, Szalay AA (2003) Optical imaging: Bacteria, viruses, and mammalian cells encoding light-emitting proteins reveal the locations of primary tumors and metastases in animals. *Anal Bioanal Chem* 377:964–972.
12. Moss B (1996) Genetically engineered poxviruses for recombinant gene expression, vaccination, and safety. *Proc Natl Acad Sci USA* 93:11341–11348.
13. Lin S-F, et al. (2007) Treatment of anaplastic thyroid carcinoma in vitro with a mutant vaccinia virus. *Surgery* 142:976–983.
14. Kelly KJ, et al. (2008) Novel oncolytic agent GLV-1h68 is effective against malignant pleural mesothelioma. *Hum Gene Ther* 19:774–782.
15. Chakrabarti S, Sisler JR, Moss B (1997) Compact, synthetic, vaccinia virus early/late promoter for protein expression. *Biotechniques* 23:1094–1097.
16. Gnant MF, Puhlmann M, Alexander HR, Jr, Bartlett DL (1999) Systemic administration of a recombinant vaccinia virus expressing the cytosine deaminase gene and subsequent treatment with 5-fluorocytosine leads to tumor-specific gene expression and prolongation of survival in mice. *Cancer Res* 59:3396–3403.
17. Kaufman HL, et al. (2005) Targeting the local tumor microenvironment with vaccinia virus expressing B7.1 for the treatment of melanoma. *J Clin Invest* 115:1903–1912.
18. Okada H, Wakamiya N, Okada N, Kato S (1987) Sensitization of human tumor cells to homologous complement by vaccinia virus treatment. *Cancer Immunol Immunother* 25:7–9.
19. Kobayashi H, Lin PC (2006) Antiangiogenic and radiotherapy for cancer treatment. *Histol Histopathol* 21:1125–1134.
20. Yamamoto Y, et al. (1996) Concentrations of vascular endothelial growth factor in the sera of normal controls and cancer patients. *Clin Cancer Res* 2:821–826.
21. Veeravagu A, et al. (2007) Vascular endothelial growth factor and vascular endothelial growth factor receptor inhibitors as anti-angiogenic agents in cancer therapy. *Recent Patents Anti-Cancer Drug Discovery* 2:59–71.
22. Harper J, Moses MA (2006) Molecular regulation of tumor angiogenesis: Mechanisms and therapeutic implications. *EXS* 96:223–268.
23. Quesada AR, Medina MA, Alba E (2007) Playing only one instrument may be not enough: Limitations and future of the antiangiogenic treatment of cancer. *Bioessays* 29:1159–1168.
24. Gerber HP, Kowalski J, Sherman D, Eberhard DA, Ferrara N (2000) Complete inhibition of rhabdomyosarcoma xenograft growth and neovascularization requires blockade of both tumor and host vascular endothelial growth factor. *Cancer Res* 60:6253–6258.
25. Ebos JM, Lee CR, Christensen JG, Mutsaers AJ, Kerbel RS (2007) Multiple circulating proangiogenic factors induced by sunitinib malate are tumor-independent and correlate with antitumor efficacy. *Proc Natl Acad Sci USA* 104:17069–17074.
26. Fischer C, et al. (2007) Anti-PlGF inhibits growth of VEGF(R)-inhibitor-resistant tumors without affecting healthy vessels. *Cell* 131:463–475.
27. Kerbel RS (2008) Tumor angiogenesis. *N Engl J Med* 358:2039–2049.
28. Smirne C, Camandona M, Rosso E, Bellone G, Emanuelli G (1999) Vascular endothelial growth factor. From basic research to clinical application. *Minerva Med* 90:15–23 (Italian).
29. Tromp SC, et al. (2000) Tumor angiogenesis factors reduce leukocyte adhesion in vivo. *Int Immunol* 12:671–676.
30. Gabrilovich DI, Ishida T, Nadaf S, Ohm JE, Carbone DP (1999) Antibodies to vascular endothelial growth factor enhance the efficacy of cancer immunotherapy by improving endogenous dendritic cell function. *Clin Cancer Res* 5:2963–2970.
31. Mantovani A, Romero P, Palucka AK, Marincola FM (2008) Tumour immunity: Effector response to tumour and role of the microenvironment. *Lancet* 371:771–783.
32. Thorne SH, Bartlett DL, Kirn DH (2005) The use of oncolytic vaccinia viruses in the treatment of cancer: A new role for an old ally? *Curr Gene Ther* 5:429–443.
33. Waine GJ, et al. (1994) Purification of a recombinant Schistosoma japonicum antigen homologous to the 22-kDa membrane-associated antigen of S. mansoni, a putative vaccine candidate against schistosomiasis. *Gene* 142:259–263.
34. Falkner FG, Moss B (1990) Transient dominant selection of recombinant vaccinia viruses. *J Virol* 64:3108–3111.
35. Joklik WK (1962) The purification of four strains of poxvirus. *Virology* 18:9–18.
36. Weibel S, Stritzker J, Eck M, Goebel W, Szalay AA (2008) Colonization of experimental murine breast tumours by Escherichia coli K-12 significantly alters the tumour microenvironment. *Cell Microbiol* 10:1235–1248.
37. Weidner N, Semple JP, Welch WR, Folkman J (1991) Tumor angiogenesis and metastasis—correlation in invasive breast carcinoma. *N Engl J Med* 324:1–8.